Synthesis and optimization of peptidomimetics as HIV entry inhibitors against the receptor protein CD4 using STD NMR and ligand docking†

Axel T. Neffe, Matthias Bilang and Bernd Meyer*

Received 18th April 2006, Accepted 20th June 2006
First published as an Advance Article on the web 26th July 2006
DOI: 10.1039/b605380g

We recently described the design and synthesis of a novel CD4 binding peptidomimetic as a potential HIV entry inhibitor with a K_D value of ~35 μM and a high proteolytic stability [A. T. Neffe and B. Meyer, *Angew. Chem., Int. Ed.*, 2004, **43**, 2937–2940]. Based on saturation transfer difference (STD) NMR analyses and docking studies of peptidomimetics we now report the rational design, synthesis, and binding properties of 11 compounds with improved binding affinity. Surface plasmon resonance (SPR) resulted in a $K_D = 10$ μM for the best peptidomimetic **XI**, whose binding affinity is confirmed by STD NMR ($K_D = 9$ μM). The STD NMR determined binding epitope of the ligand indicates a very similar binding mode as that of the lead structure. The binding studies provide structure activity relationships and demonstrate the utility of this approach.

Introduction

The first step in the infection of a human cell with HIV is the interaction between the viral envelope glycoprotein gp120 and human CD4.[1] After this event, gp120 interacts with a coreceptor,[2] normally CCR5 or CXCR4[3] to infect the human cell.[4] The three main classes of clinical anti HIV drugs, *i.e.* nucleoside reverse transcriptase inhibitors (NRTIs), non nucleoside reverse transcriptase inhibitors (nNRTIs), and protease inhibitors (PIs) inhibit viral replication after infection of the cell.[5] Despite advances in HIV treatment,[6] none of these drugs nor their combination can finally cure HIV infection.[7] Due to the high mutation rate of HIV and the resulting resistance against drug treatment,[8] new classes of drugs have to be developed.[9]

A promising concept is the inhibition of one of the interactions resulting in membrane fusion.[10] These—so called—entry inhibitors could assist in HIV treatment as is demonstrated by the success of fuzeon (enfuvirtide, T20).[11] Likewise, other compounds preventing receptor or coreceptor binding of the virus could potentially be utilized as HIV medication.[12]

Targeting the interaction of gp120 with CD4, others developed gp120 or antibody related peptides,[13] or gp120 binding molecules.[14] The approach of developing CD4 ligands might potentially interfere with the human immune system, as CD4 plays an important role in the binding of MHC class II proteins to T cell receptors.[15] The region on the CD4 protein that binds to gp120 is overlapping the one that binds to the MHC class II proteins.[16] However, the contact area of the gp120–CD4 interaction is much larger (and therefore stronger) than that of the CD4–MHC class II protein interaction.[17]

On the other hand, blocking the CD4 protein on the human cell is much less likely to cause viral resistance. In order to become resistant to a CD4 binding drug, the virus would have to switch to a totally different entry mechanism to infect macrophages and T-cells. However, this is not very probable as it would require the mutation of many amino acids simultaneously forcing the virus to establish a new and highly efficient entry mechanism.

We reported a peptidomimetic compound **I** (*cf.* Fig. 1),[18] derived from the known CD4 binding peptide NMWQKVGTPL that shows an antiviral activity in an HIV proliferation assay.[19] This was achieved by eliminating all amino acids of the lead compound that do not contribute to binding, *i.e.* asparagine, methionine, and glutamine. The two hydrophobic amino acids tryptophane and leucine were replaced by generic hydrophobic non amino acid residues. Additionally, non peptidic linkages have been incorporated. **I** shows a 170 fold stronger binding ($K_D = 35$ μM) to CD4 than the original peptide, a 4–5 times higher proteolytic stability, and a lower molecular weight of ≈800 compared to the lead peptide. Therefore, **I** has much better pharmacological properties compared to the lead decapeptide NMWQKVGTPL.

Here we describe the optimization of the pharmacological properties of this class of compounds. Starting from the lead peptide we docked about 85 peptidomimetics that were created by changing one residue at a time to test for the optimal residues at each position. Of these, eleven compounds were chosen for synthesis and nine of them were fully characterized by 2D NMR techniques. The binding affinities of all substances to CD4 were determined by surface plasmon resonance (SPR), the best compound in this assay was also analyzed with saturation transfer difference (STD) NMR for its K_D and binding epitope. The combined results gave information about structure activity relationships.

Results and discussion

Docking

Extensive docking studies were performed using the program Flexidock of the Sybyl (version 6.9) software package (Tripos, Inc.). Due to the simplifications of the docking procedure, *e.g.*

Institute for Organic Chemistry, University of Hamburg, Martin Luther King Platz 6, 20146, Hamburg. E-mail: bernd.meyer@chemie.uni-hamburg.de, axel@neffe.org; Fax: +49 40 428382878

† Electronic supplementary information (ESI) available: SPR graphs, characterization data and docking results of the compounds with variation of the aromatic residues. See DOI: 10.1039/b605380g

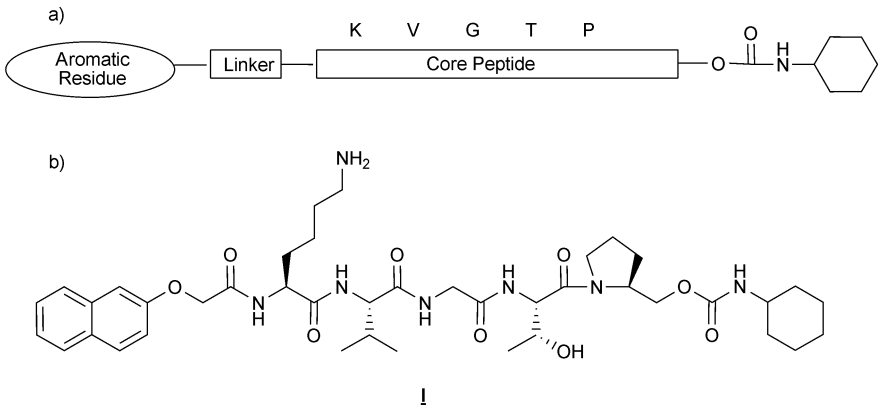

I

Fig. 1 a) The template on which the design of the newly synthesized peptidomimetics is based. The peptidomimetics consist of a core pentapeptide carrying non-peptidic, hydrophobic residues on the *N*- and *C*-termini. b) Structure of the peptidomimetic **I** with a $K_D = 35\ \mu M$.

no consideration of solvent effects, the calculated binding energies can only be regarded as semi quantitative indicators of the binding affinity. The docked model of **I** (Fig. 2) served as starting position for docking studies of other ligands. First the corresponding functional group(s) were replaced and, subsequently, the resulting structures were minimized for a short period each. The docking results were interpreted in terms of the existing experimental data, like X-ray analyses, STD NMR, and binding studies for related compounds.

In the docking process, we studied different aromatic residues, different linkages between the aromatics and the core peptide, as well as different amino acids forming the core of the peptidomimetics (*cf.* Fig. 1a) to improve the affinity of **I**. The *N*-terminal linker and the aromatic residues were selected during the design phase of the template without consideration of the cyclohexylcarbamoyl subunit at the C-terminus. After selection the complete peptidomimetics were docked and their energy evaluated.

A variety of aromatic ring systems, selected by similarity search in the available chemicals directory (ACD), were docked to potentially improve the effect of the β-naphthyl residue. Compounds with a quinolyl and 4-methylcoumarin group on the *N*-terminus showed calculated binding affinities close to that of the original aromatic β-naphthyl system and were therefore chosen for synthesis, as was the α-naphthyl derivative to elucidate the ideal substitution pattern at the aromatic ring (*cf.* **II**, **III** and **IV**, Chart 1). Compounds with an isoquinoline, benzodiazole, benzothiazole, indole, or biphenyl group on the *N*-terminus did not show favorable interactions with CD4 in the docking experiments (details see supporting information†).

We also varied the linkers of the peptidomimetics that connect the core peptide and the aromatic ring (*cf.* Fig. 3). The best interaction energies were observed for the oxyacetic acid linker **1** and for similar longer linkers **6a** and **7**, *cf.* Table 1. Because of

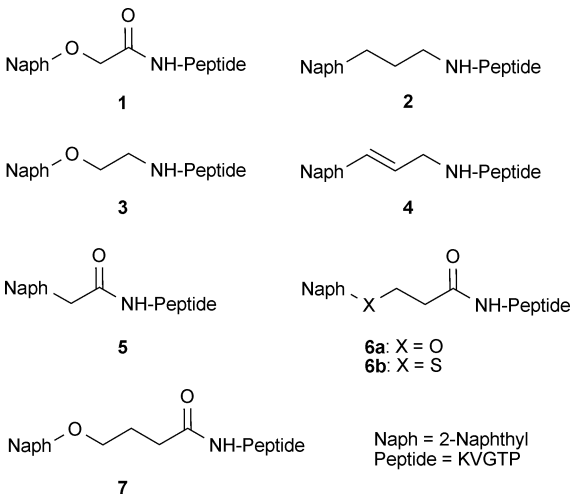

Fig. 3 Different types of linkers analyzed in the docking.

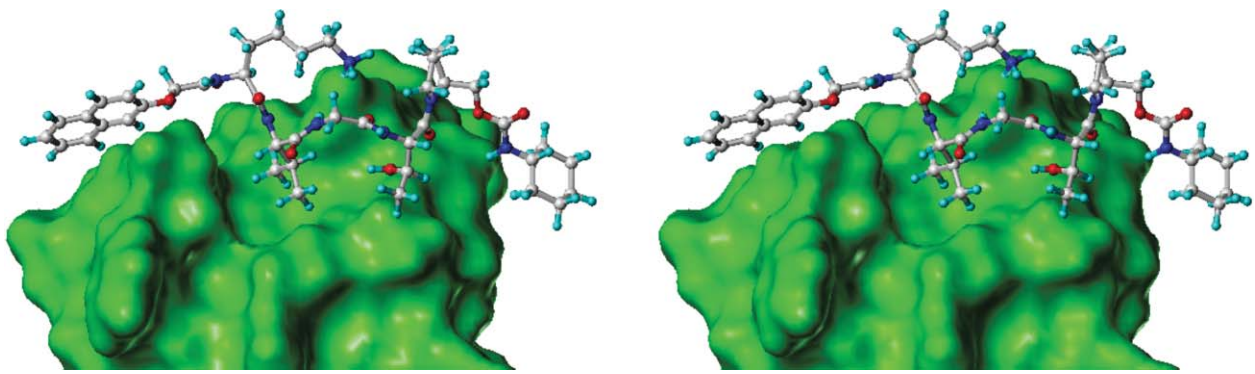

Fig. 2 Stereo view of the docked ligand **I** shown as ball and stick on the surface of the CD4 protein (green). The excellent complementarity of the surface to the ligand is clearly visible.

 This journal is © The Royal Society of Chemistry 2006

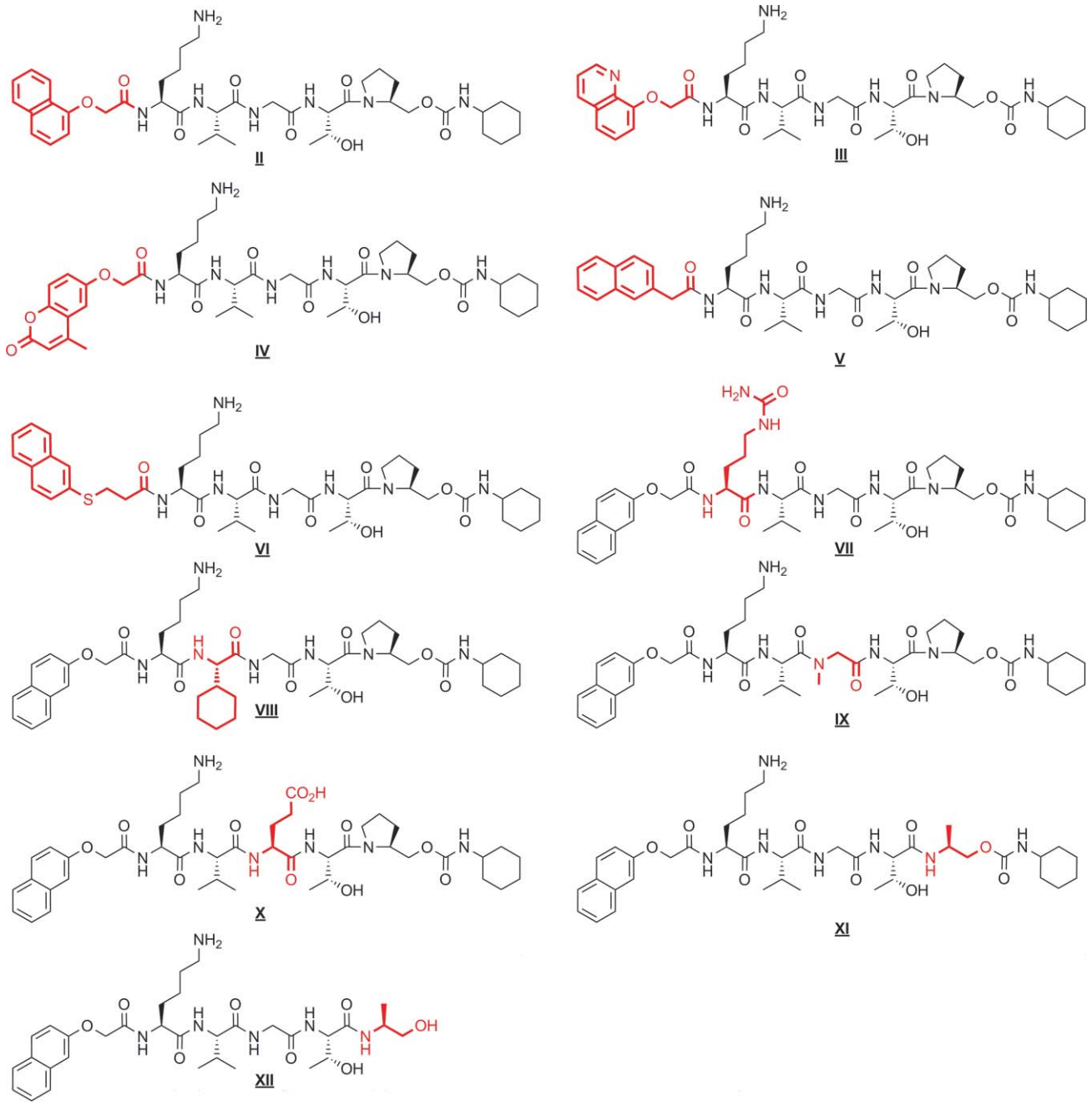

Chart 1 Structures of the peptidomimetics **II–XII**.

Table 1 Calculated binding energies of the ligand–protein complexes of peptidomimetics with different linkages and energy differences relative to the oxyacetic acid linker

Linker	Energy/kcal mol^{-1}	ΔE/kcal mol^{-1}
1	−274	0
2	−264	10
3	−261	13
4	−258	16
5[a]	—	—
6a	−292	−18
7	−290	−16

[a] For this compound, no binding energy could be determined, because of spatial separation of the ligand protein complex during docking.

these findings and the ease of synthesis, an amide bond between the core and the aromatic residue was chosen for synthesis. The three atom linker of **1** seemed to be a good compromise between the right distance and flexibility, even though the longer linkers gave a better score. To validate this hypothesis, two compounds with the linkers **5** and **6b** were synthesized (*cf.* **V** and **VI**). **6b** was chosen as it was commercially available contrary to **6a**.

The lysine of the peptidomimetic **I** shows a tight interaction with Asp_{63} of CD4 in docking experiments (Fig. 4). Side chains without a terminal basic functional group at this position lead to a complete loss of the binding affinity. Therefore, histidine, arginine and citrulline were tested as potential replacements for the lysine residue. The side chain of histidine is too short to interact with

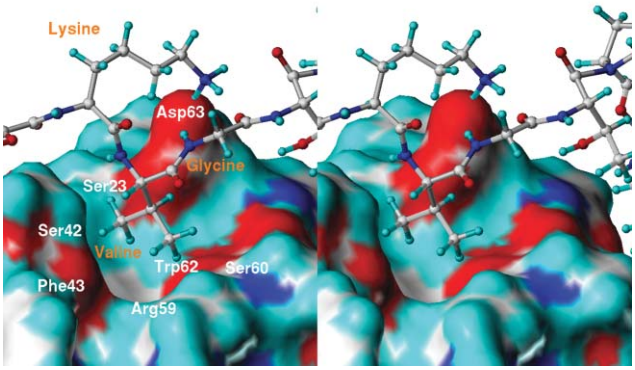

Fig. 4 Stereo view of the interaction of the lysine, valine and glycine of **I** (ball and stick) with CD4 (shown as a surface with the patches of the surface carrying the color of the associated atoms; red: oxygen, blue: nitrogen, cyan: hydrogen, white: carbon).

Asp_{63}. Arginine and citrulline were estimated to have roughly equal binding energies, despite having different pK_B values. We decided to synthesize the citrulline containing compound, because of the expected higher proteolytic stability (*cf.* **VII**, Chart 1).

Valine fits into a hydrophobic cavity formed of Trp_{62}, Ser_{42}, Phe_{43}, Arg_{59}, Ser_{60}, and Ser_{23} (Fig. 4). To some degree this cavity is flexible and there may be place for bigger hydrophobic residues.[20] Therefore, a peptidomimetic in which cyclohexylglycine (Chg) substitutes for valine was synthesized (*cf.* **VIII**, Chart 1).

The glycine does not show a direct interaction with CD4 in the STD NMR experiments of **I**. Therefore, it was an obvious candidate for substitution (Fig. 4). An alanine substitution leads to a reduced calculated binding affinity. Alternatively, peptidomimetics containing amino acids with a basic (histidine) and an acidic (glutamate) side chain in this position were docked. While the incorporation of histidine resulted in a lower calculated binding affinity, glutamate increases the calculated binding affinity because of a possible interaction with Ser_{60} of the CD4 (*cf.* **X**, Chart 1). Since the amidic proton of glycine is not participating in hydrogen bonding to CD4, the substitution with sarcosine should not have a significant influence on the binding energy but could increase proteolytic stability (*cf.* **IX**, Chart 1).

Interactions of threonine and prolinol with CD4 are predicted by Flexidock (*cf.* Fig. 5). All attempts to substitute the threonine residue led to a worse binding energy. The *in silico* alanine scan of the lead peptide showed that substitution of proline with alanine resulted in a better binding energy. Therefore, we replaced prolinol with alaninol (*cf.* **XI**, Chart 1).

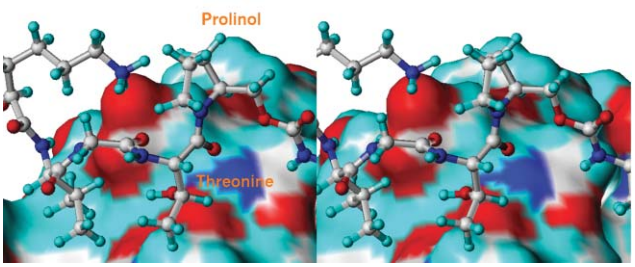

Fig. 5 Stereo view of threonine and proline of **I** binding to CD4 in the docking. The intensity of the proline Hβ protons observed in the epitope mapping is not explained by this model.

Synthesis and characterization

Chart 1 shows all synthesized peptidomimetics. All building blocks were purchased in the highest possible purity. (8′-Quinolyloxy)acetic acid, (1′-naphthyloxy)acetic acid, and (6′-(4′-methyl)coumarinyloxy)acetic acid were synthesized by Williamson ether synthesis of the respective aromatic alcohol and bromo acetic acid.[21] The peptidomimetics were synthesized in parallel, following the published procedure as shown in Scheme 1 for **I**.[18] The solid phase synthesis gave yields for the unpurified primary alcohol of 20–35% (equivalent to 72–80% per coupling–deprotection cycle). The relatively low yields are due to problematic coupling reactions connecting to the sterically demanding prolinol and valine residues, respectively. The carbamates at the C-terminus were formed in 62–80% yield. Deprotection and RP-HPLC purification resulted in overall yields of 1–7% of isolated product, respectively. **XII** (Chart 1) was the result of an incomplete coupling of the isocyanate[22] and was also tested for binding affinity. For the peptidomimetic **I**, two stable conformers could be detected by 2D NMR spectra.[18] The same findings were obtained for **II–X**. However, this equilibrium was not observed for **XI** and **XII** which both have an alaninol subunit substituting for the prolinol. This reinforces the assumption that the conformers are the *cis* and *trans* rotamers, respectively, of the threonine prolinol amide bond.

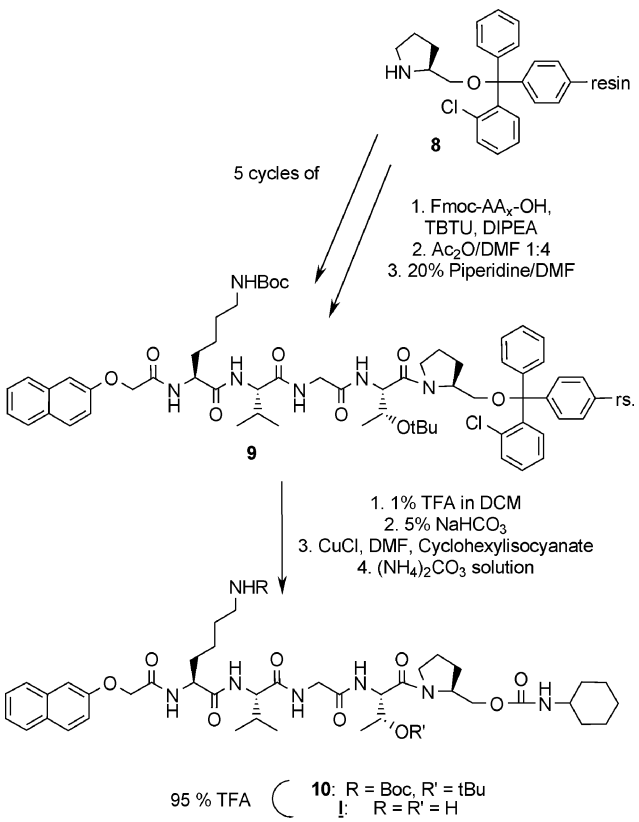

Scheme 1 Synthesis of the peptidomimetics as exemplified for **I**.

SPR analysis

The K_D-values of all substances have been determined by SPR. The compounds were passed over a Biacore CM5 chip with immobilized CD4. About 53 fmol (44 fmol for **V** and **VI**, respectively) of

This journal is © The Royal Society of Chemistry 2006

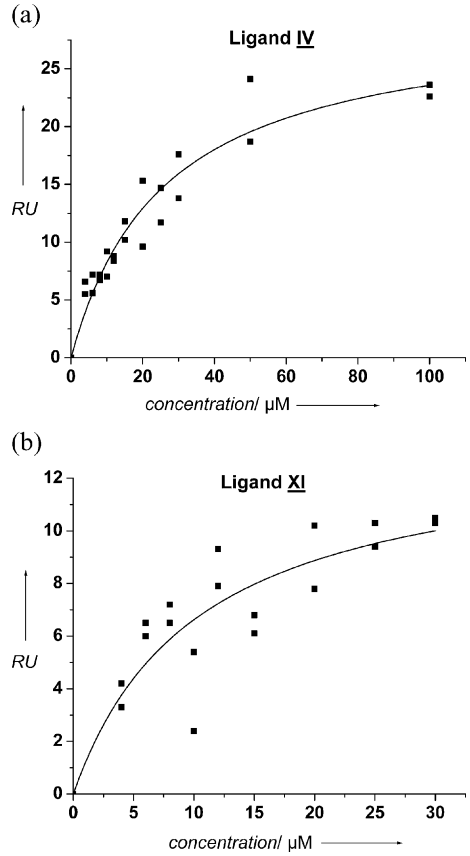

Fig. 6 Fit of the SPR data points to a one site binding model of the compounds **IV** ($K_D = 26$ μM) and **XI** ($K_D = 10$ μM). The data show the results from two independent concentration dependent SPR experiments. Response units (RU) given by the SPR experiment are directly correlated to the amount of ligand bound (1 RU is approximately equivalent to 1 pg of substance).

CD4 were active after immobilization. A concentration dependent binding assay with 4, 6, 8, 10, 12, 16, 20, 25, 30, 50, 100, 500 and 1000 μM of the corresponding ligand in buffer was performed. The data points of the lower concentrations of all ligands can be fitted to a one-site binding model, while for higher concentrations a linear correlation of the binding affinity with the concentration was found. This behaviour indicates a non specific (*i.e.* non saturable) binding, resulting from secondary binding sites on the protein of very low affinity or aggregation of the ligands at higher concentrations. K_D values were therefore determined only with the data points following a saturable binding behaviour. Regression of these data points using a one-site binding model to eqn (3) yielded the binding constants. All data are presented in Table 2. The results of the binding assays for **IV** and **XI** are depicted in Fig. 6, the others are shown in the supporting information†. In general, the fit is good, with exception of **VI**, whose data points have a great variance (see supporting information†).

The best compound in this assay, **XI**, has a K_D value of 10 μM, which is about 4-fold better than that of **I** ($K_D = 39$ μM from SPR, $K_D = 31$ μM from STD NMR) and 600 fold better than the lead NMWQKVGTPL ($K_D = 6$ mM). The k_{on} and k_{off} values could be determined by the analysis of individual SPR curves. The k_{on} values for the peptidomimetics range from 6×10^3 s^{-1} M^{-1} to 3×10^4 s^{-1} M^{-1}, while k_{off} is about 0.1–0.2 s^{-1}. This is a relative slow binding kinetic, possibly indicating an induced fit and/or conformational changes of the ligand.

Table 2 The calculated binding energies from the docking and the respective experimental K_D values including the standard deviation of the newly synthesized peptidomimetics **II–XII** in comparison to **I**. The structures of **II–XII** are shown in Chart 1. Also shown is the highest concentration that was used for the regression analysis. Depending on the hydrophobic nature of the peptidomimetics **I–XII**, aggregation and thus unspecific binding starts at different concentrations for each molecule thus requiring different cut-offs for the calculation of the binding constant

Compound	Calculated binding energy/kcal mol^{-1}	K_D/μM	Highest fitted concentration/μM
I	−376	39 ± 5	32
III	−370	55 ± 19	30
III	−379	16 ± 4	30
1V	−382	26 ± 4	100
V	−374	105 ± 33	100
VI	−376	53 ± 102	25
VII	−344	31 ± 6	50
VIII	−334	146 ± 94	50
IX	−387	26 ± 5	100
X	−400	30 ± 7	30
XI	−372	10 ± 4	30
XII	−359	103 ± 50	500

STD NMR

The most promising compound **XI** has been analyzed in detail by 1D ^{1}H-STD NMR spectroscopy (Fig. 7 and 8).[23] The K_D values (Table 3) determined by this homogeneous NMR based method are in good agreement with the value obtained by the

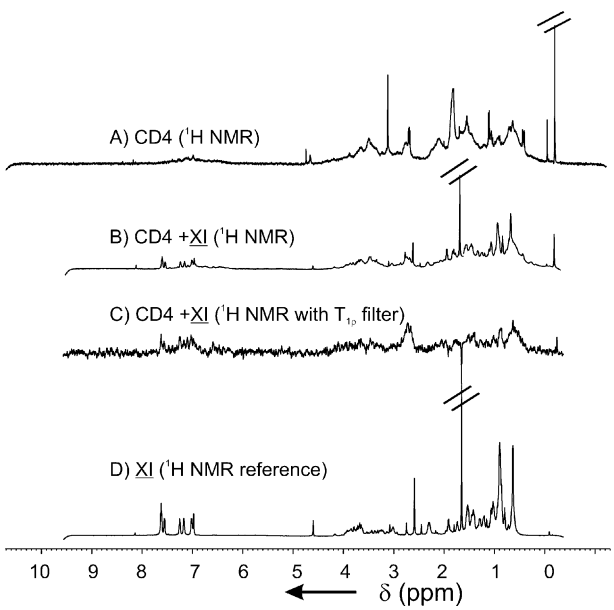

Fig. 7 a) ^{1}H NMR spectrum of CD4. The typical broad lines for proteins are observed with a few sharp signals resulting from amino acids on the surface of CD4. b) ^{1}H NMR spectrum of a mixture of 4.4 μM CD4 and 75 μM **XI** containing 20 μM DSS as internal standard. c) Corresponding ^{1}H STD NMR spectrum of the same sample with $T_{1\rho}$ filter for the reduction of most protein signals. Most of the remaining signals could be identified as signals of **XI**. A titration experiment with different concentrations of the ligand was used to determine K_D. d) ^{1}H NMR reference spectrum of **XI**.

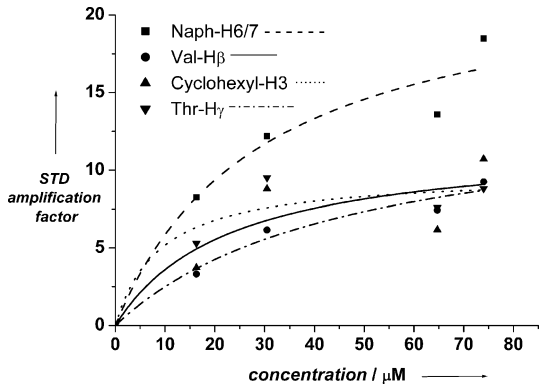

Fig. 8 STD NMR titration curves for a choice of individual protons of **XI**. All data are presented in Table 3.

heterogeneous SPR system. The different values for individual protons are due to varying distances to the protein surface and because of diverse relaxation times of the protons. K_D values from those protons yielding the lowest K_D values and thus having the tightest binding to the receptor are presented. This results in a K_D value of 9 μM by STD NMR in comparison to 10 μM by SPR.

The most intensive peaks in the 1D STD NMR ^{1}H NMR spectrum were used to derive the binding epitope of the ligand, which is shown in Fig. 9 and is further visualized in Fig. 10 and 11.

Table 3 K_D values of individual protons of **XI**, calculated through a regression analysis of the data points of the STD NMR titration by fitting a one site binding model

Proton	K_D/μM
Naph-H4/5/8	12
Naph-H6/7	30
Naph-H1/3	16
Val-Hβ	47
Cyclohexyl-H4	35
Cyclohexyl-H3	23
Thr-Hγ	9
Val-Hγ	25

It shows comparable regions of the molecule to be in close contact to CD4 as in the lead peptide NMWQKVGTPL and in **I**.[18]

Structure activity relationships

The analysis of the K_D values and the docking results provide insight into structure activity relationships (for ligand structures see Chart 1). Aromatic systems containing hetero atoms (**III** and **IV**) bind better than **I**. Also, by comparing the K_D values of **I** and **II** it becomes clear that β-naphthyl residues bind better than α-naphthyl residues. The oxyacetic acid linker proved to be the best choice accommodating the requirements for distance and

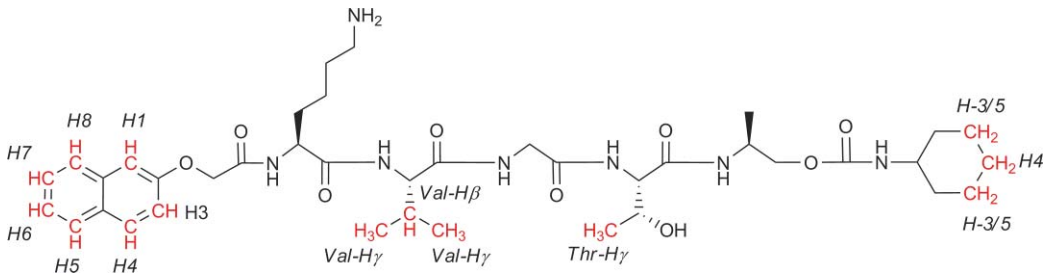

Fig. 9 Ligand epitope mapping of **XI**. Highlighted protons shown in red are in close contact to CD4.

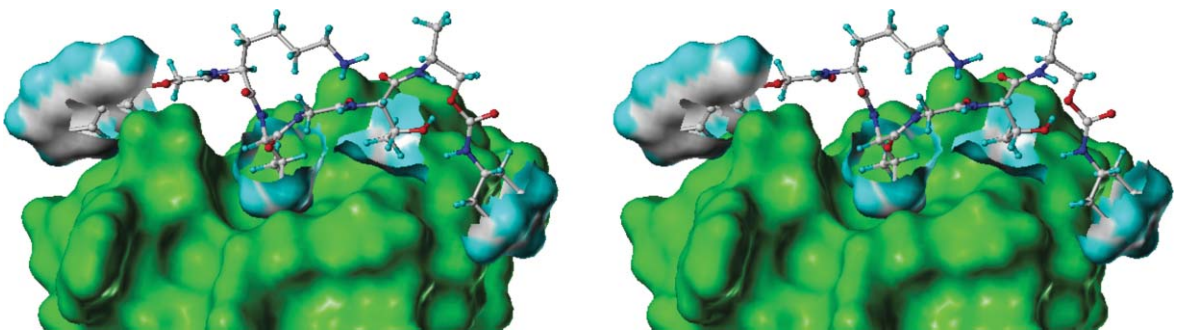

Fig. 10 **XI** (ball and stick, with the atom colored surface of the binding epitope) docked to CD4 (green).

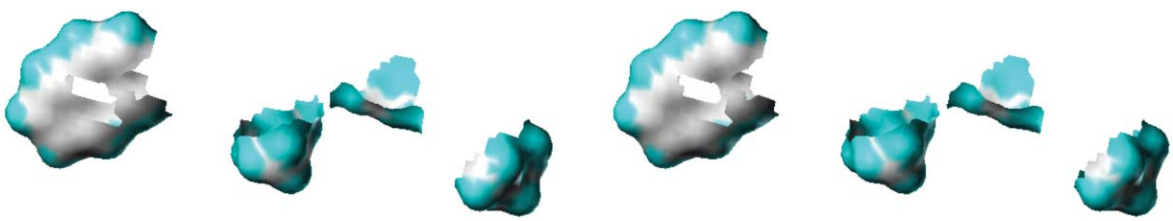

Fig. 11 The surface of the binding epitope of **XI** determined by ^{1}H STD NMR. In fact, only these parts of the ligand are needed for binding.

 This journal is © The Royal Society of Chemistry 2006

flexibility as is obvious from the binding affinity of **I**, **V**, and **VI**. This was already suspected during the design stage. Compound **VII** containing citrulline instead of lysine binds slightly better than **I**. The worst binding affinity was measured for **VIII**, indicating that the hydrophobic cavity that normally encloses the valine residue is not large enough for the cyclohexyl residue. Glycine may be substituted by either sarcosine or glutamate to improve the binding affinity slightly, while the replacement of prolinol with alaninol in **XI** clearly results in an improved binding affinity. This is partly due to the fact that **XI** has only one stable conformer in solution. The 10 fold decrease in binding affinity of **XII** in comparison to **XI** shows the importance of the cyclohexylcarbamoyl group. Further modifications of this carbamoyl residue may result in even better binding compounds.

Experimental

Synthesis

Synthesis of the (aryloxy)acetic acids. 1 eq. aromatic alcohol was refluxed in ethanol (2 mL mmol^{-1}). A solution of KOH (2.17 eq.) in ethanol (0.8 mL mmol^{-1}) was added and subsequently a solution of bromo acetic acid (1.03 eq.) in ethanol (0.5 mL mmol^{-1}) was added dropwise. The solution was cooled down to room temperature and stirred for another 12 hours ((8-quinolyloxy)acetic acid forms a colorless precipitate during this time and can be used without further workup). The ethanol was evaporated, the residue dissolved in 20 mL ethyl acetate and extracted three times with 10 mL of 5% aqueous $NaHCO_3$. The combined aqueous phases were acidified with conc. HCl to pH 2–3 and extracted three times with 10 mL ethyl acetate. The organic layer was dried over $MgSO_4$ and the solvents were evaporated. Drying in high vacuum gave the desired product which needed no further purification.

(1′-Naphthoxy)acetic acid. 1.3 g (6.4 mmol) (1′-naphthoxy)-acetic acid (46.5%) as colorless solid, mp 194–196 °C (Lit: 193–195 °C); δ_H (400 MHz, MeOH-d_4) 8.39–8.34 (1H, m, H8), 7.87–7.82 (1H, m, H5), 7.55–7.47 (3H, m, H4/6/7), 7.43–7.37 (1H, m, H3), 6.89–6.85 (1H, m, H2), 4.89 (2H, s, CH_2); δ_C (400 MHz, MeOH-d_4–$CDCl_3$ 2 : 1) 175.2 (CO_2H), 154.9 (C1), 134.9 (C4a), 127.7 (C5), 126.9 (C6), 125.9 (C3), 125.7 (C7), 124.8 (C8a), 122.4 (C8), 121.8 (C4), 105.4 (C2), 65.9 (CH_2); *m/z* (%) 202 (95), 143 (100), 127 (15), 115 (58), 77 (12), 40 (18).

6-Carboxymethoxy-4-methylcoumarin. 0.5 g (2.1 mmol) 6-carboxymethoxy-4-methylcoumarin (18.7%) as colorless solid, mp 104–106 °C; δ_H (400 MHz, MeOH-d_4) 7.38–7.26 (3H, m, H5/7/8), 6.39 (1H, d, $^4J_{H3-CH3}$ 1, H3), 4.80 (2H, s, CH_2), 2.51 (3H, d, $^4J_{H3-CH3}$ 1, CH_3); δ_C (400 MHz, MeOH-d_4) 121.3 (C5), 119.3 (C7), 116.2 (C8), 110.8 (C3), 19.1 (CH_3); *m/z* (%) 234 (100), 175 (50), 147 (69), 91 (18).

(8-Quinolyloxy)acetic acid. 0.7 g (3.4 mmol) (8-quinolyloxy)-acetic acid (24.6%) as yellow solid, mp 168 °C; δ_H (400 MHz, MeOH-d_4) 9.27 (1H, m, H2), 9.24 (1H, m, H4), 8.21 (1H, m, H3), 8.02–7.92 (2H, m, H5 + H6), 7.73 (1H, m, H7); *m/z* (%) 203 (3), 158 (100), 145 (8), 129 (55), 102 (15), 89 (10).

Synthesis of the peptidomimetics

The synthesis of the peptidomimetics has been described before.[18] The synthesis starts with an amino alcohol linked to a 2′-chlorotrityl resin *via* the hydroxy function. The following amino acids are coupled using standard peptide coupling protocols (activation by TBTU–DIPEA, Fmoc as *N*-terminal protecting group and Boc and *t*Bu, respectively, as side chain protecting groups). The coupling of the terminal carboxylic acid was accomplished in the same way *via* a normal amide bond. Mild acidic conditions (1% TFA in DCM) cleave the molecule from the resin and result in a side chain protected free alcohol. The alcohol function reacts under copper(I) catalysis with cyclohexyl isocyanate forming a carbamate linkage to give the protected peptidomimetics. Subsequent treatment with 95% TFA gives the unprotected peptidomimetic, which all have been characterized by MALDI TOF MS. Overall yield of the products was 1–7% after HPLC purification. All NMR data of **II**, **III** and **V–XI** are shown in the supporting information†, **IV** and **XII** have not been characterized by NMR due to low yield.

Experimental details of the docking

Docking studies were carried out on Silicon Graphics Octane or Octane2 computers using the program Flexidock of the Sybyl (version 6.9) software package (Tripos, Inc.). The structure of CD4 was obtained from a Protein Data Bank file (code 1gc1.pdb)[2b] and was treated as described before.[18] The force field calculations take into account van der Waals, electrostatic, torsional, and constraint energy terms. All bonds of the ligand were freely rotatable, as well as the amino acids of the CD4 binding epitope to allow an induced fit docking.

Experimental details of SPR experiments

The SPR data were determined on a BIACORE 3000 instrument using CM5 chips. 106 fmol and 220 fmol, respectively, sCD4 were covalently attached to the activated dextrane matrix. The surface was activated by *N*-hydroxysuccinimide and *N*-(3-dimethylaminopropyl)-*N*-ethylcarbodiimide hydrochloride for the coupling of the protein. After coupling of the protein the matrix was capped with ethanolamine. The activity of the immobilized protein was checked by gp120 binding; extrapolation of the data showed an activity of 50% (53 fmol) and 20% (44 fmol), respectively, of the immobilized CD4.[24] sCD4 was obtained from Progenics Pharmaceuticals, Tarrytown, New York, USA. Catalogue-No.: PRO1008-1, Lot 48 (recombinant human soluble CD4 (CHO), purity >95%, amino acids 1–370 of the natural CD4 (45 kDa)), gp120 was purchased from the National Institute for Biological Standards and Control, catalogue-No. EVA607, http://www.nibsc.ac.uk/catalog/ aids-reagent (recombinant HIV-1 IIIB GP120, 120 kDa. purity >95%, expression system: baculovirus). The K_D value of the gp120–CD4 interaction is in the low nM range (depending on the method).[2b,25] The activity was calculated following eqn (1) and (2).

$$\text{activity (CD4)} = \frac{\text{RU[gp120] max}_{\text{measured}}}{\text{RU[gp120] max}_{\text{calculated}}} \quad (1)$$

$$\text{active CD4 [fmol]} = \text{activity (CD4)} \times \text{immobilized CD4 [fmol]} \quad (2)$$

We used a dilution series with concentrations of the peptidomimetics of 4, 6, 8, 10, 12, 16, 20, 25, 30, 50, 100, 500 and 1000 μM in HBS-EP (10 mM HEPES, 150 mM NaCl, 3 mM EDTA, 0.005% surfactant P20, pH 7.4) buffer. Contact time was 120 s with a flow rate of 15 μL min^{-1} and a dissociation time of 60 s. Every concentration was measured twice starting from the lowest concentration. The surface was regenerated with two injections of 100 mM H_3PO_4 for 32 s with the same flow rate. The dependence of the response units (RU; 1 RU ~ 1 pg) on the concentration can be used to obtain K_D values using eqn (3):

$$\mathrm{RU}([c]) = \frac{[c]\,\mathrm{RU}_{max}}{K_D + [c]} \quad (3)$$

The RUs for each ligand and concentration were determined by subtracting the RUs of pure buffer solutions (blanks) from the individually observed RUs. The peptidomimetics did not show an asymptotic behavior at high concentrations in the Biacore assay. This may be due to unspecific binding of the ligands to the protein surface or because of a second binding site with a lower binding affinity. Therefore, only data points representing a typical association curve were used for data analysis (*cf.* Table 3).

Experimental details of STD NMR experiments

Preparation of the samples. Commercially available sCD4 (see above) (200 μg, 4.4 nmol) was dissolved in buffer (200 μL D_2O, containing 8 mM Na_2HPO_4, 2 mM NaH_2PO_4, 140 mM NaCl, 3 mM KCl and 6 mM NaN_3, adjusted to pH = 7–7.5 (not corrected) with 0.1 M DCl). Through repeated dilution and membrane centrifugation, the sample was rebuffered in deuterated PBS, resulting in 250–300 μL solution (exactly measured by weighing). The protein solution was split into two halves and 5 μL 1 mM DSS solution in D_2O was added to each portion. The samples were filled to 250 μL each, one with buffer and the other one with buffer containing **XI** to produce the highest concentration of 80 μM. The samples were transferred into Shigemi NMR tubes and measured on a Bruker Avance 700 MHz spectrometer with a cryo probe. The other concentrations of the ligand were achieved by diluting the ligand solution with the buffered protein solution from the other sample and *vice versa*. The exact concentrations of the ligand were determined by comparison with the internal DSS standard.

The *on resonance* frequency was determined by measuring the ligand sample only. At −1.5 ppm, all discoverable artefacts were ≪1 rel. STD%. The number of scans of the reference spectra and the STD spectra was adjusted to the concentration and was up to 11k for the STD spectrum at the lowest ligand concentration of 16 μM. The off resonance frequency was at 28.6 ppm.

Data analysis. The 1D ^{1}H NMR spectra were acquired at a spectral width of 10 ppm and with 32k data points. Before Fourier transformation, these were filled up to 64k with zeros. Through multiplication of the FID with an exponential function (line broadening: 5 Hz), an increase of the signal noise ratio was achieved, and subsequently the phase was corrected. A $T_{1\rho}$ filter of 15 ms with an attenuation of 12 dB eliminated nearly all protein signals. The phase cycle of the STD experiments was selected, such that the subtraction needed for the difference spectra occurred on alternating scans. In this way, artifacts due to temperature or magnetic inhomogeneities are minimized. On- and off-resonance frequency of the presaturation pulses alternated each scan. All STD experiments were recorded with WATERGATE water suppression. For determination of the relative STD% and the STD amplification factor, a reference experiment was recorded with the same conditions, processed and phased with the same parameters. The integrals were compared in the dual display mode in XWINNMR (version 3.1, Bruker). The temperature of the samples was 285 K.

Conclusions

We could improve the binding affinity of the CD4 binding peptidomimetics and gain insight in structure activity relationships. Even though the calculated binding energies by Flexidock represent the experimental binding affinity only semi quantitatively, theoretical and analytical data show a positive correlation. Overall we could show that this protocol for a rational drug design yielded 7 out of 11 compounds with an improved binding constant compared to the lead.

Acknowledgements

This work was supported by grants from the Deutsche Forschungsgemeinschaft (DFG) through Graduiertenkolleg 464 and SFB 470/B2. We acknowledge that the AIDS reagent program of the WHO provided us with generous gifts of the CD4 and the gp120 proteins.

References

1 A. G. Dalgleish, P. C. Beverly, P. R. Clapham, D. H. Crawford, M. F. Greaves and R. A. Weiss, *Nature*, 1984, **312**, 763–767; D. Klatzmann, E. Champagne, S. Chemaret, J. Gruest, D. Guetard, T. Hercend, J. C. Gluckman and L. Montagnier, *Nature*, 1984, **312**, 767–768.
2 (*a*) Q. J. Sattentau, J. P. Moore, F. Vignaux, F. Traincard and P. Poignard, *J. Virol.*, 1993, **67**, 7383–7393; (*b*) P. D. Kwong, R. Wyatt, J. Robinson, R. W. Sweet, J. Sodroski and W. A. Hendrickson, *Nature*, 1998, **393**, 648–659.
3 A. Bjorndal, H. Deng, M. Jansson, J. R. Fiore, C. Colognesi, A. Karlsson, J. Albert, G. Scarlatti, D. R. Littman and E. M. Fenyo, *J. Virol.*, 1997, **71**, 7478–7487.
4 S. Bar and M. Alizon, *J. Virol.*, 2004, **78**, 811–820.
5 K. E. Squires, *Antiviral Ther.*, 2001, **6**(Suppl. 3), 1–14; S. Ren and E. J. Lien, *Prog. Drug Res.*, 1998, **51**, 1–31; M. Bowers, *Bull. Exp. Treat. AIDS*, 1996, **Jun.**, 19–22.
6 B. Autran, G. Carcelain, T. S. Li, C. Blanc, D. Mathez, R. Tubiana, C. Katlama, P. Debre and J. Leibowitch, *Science*, 1997, **277**, 112–116.
7 R. J. Pomerantz, *Curr. Opin. Investig. Drugs (Thomson Sci.)*, 2002, **3**, 1133–1137.
8 C. Tamalet, J. Fantini, C. Tourres and N. Yahi, *AIDS (London)*, 2003, **17**, 2383–2388.
9 J. H. Condra, M. D. Miller, D. J. Hazuda and E. A. Emini, *Annu. Rev. Med.*, 2002, **53**, 541–555.
10 M. P. D'Souza, J. S. Cairns and S. F. Plaeger, *JAMA, J. Am. Med. Assoc.*, 2000, **284**, 215–222; J. A. Turpin, *Expert Rev. Anti-infect. Ther.*, 2003, **1**, 97–128.
11 I. G. Williams, *Int. J. Clin. Pract.*, 2003, **57**, 890–897.
12 (*a*) J. M. Jacobson, I. Lowy, C. V. Fletcher, T. J. O'Neill, D. N. Tran, T. J. Ketas, A. Trkola, M. E. Klotman, P. J. Maddon, W. C. Olson and R. J. Israel, *J. Infect. Dis.*, 2000, **182**, 326–329; (*b*) C. W. Hendrix, C. Flexner, R. T. MacFarland, C. Giandomenico, E. J. Fuchs, E. Redpath, G. Bridger and G. W. Henson, *Antimicrob. Agents Chemother.*, 2000, **44**, 1667–1673.
13 (*a*) C. Boussard, V. E. Doyle, N. Mahmood, T. Klimkait, M. Pritchard and I. H. Gilbert, *Eur. J. Med. Chem.*, 2002, **37**, 883–890; (*b*) C. Monnet, D. Laune, J. Laroche-Traineau, M. Biard-Piechaczyk, L. Briant, C. Bes, M. Pugniere, J.-C. Mani, B. Pau, M. Cerutti, G. Devauchelle,

 This journal is © The Royal Society of Chemistry 2006

C. Devaux, C. Granier and T. Chardes, *J. Biol. Chem.*, 1999, **274**, 3789–3796.
14 (*a*) S. Ramurthy, M. S. Lee, H. Nakanishi, R. Shen and M. Kahn, *Bioorg. Med. Chem.*, 1994, **2**, 1007–1013; (*b*) G. P. Allaway, K. L. Davis-Bruno, G. A. Beaudry, E. B. Garcia, E. L. Wong, A. M. Ryder, K. W. Hasel, M. C. Gauduin, R. A. Koup and J. S. McDougal, *AIDS Res. Hum. Retroviruses*, 1995, **11**, 533–539.
15 J. D. Lifson and E. G. Engleman, *Immunol. Rev.*, 1989, **109**, 93–117.
16 J. H. Wang, R. Meijers, Y. Xiong, J. H. Liu, T. Sakihama, R. Zhang, A. Joachimiak and E. L. Reinherz, *Proc. Natl. Acad. Sci. USA*, 2001, **98**, 10799–10804.
17 D. G. Myszka, R. W. Sweet, P. Hensley, M. Brigham-Burke, P. D. Kwong, W. A. Hendrickson, R. Wyatt, J. Sodroski and M. L. Doyle, *Proc. Natl. Acad. Sci. USA*, 2000, **97**, 9026–9031.
18 A. T. Neffe and B. Meyer, *Angew. Chem., Int. Ed.*, 2004, **43**, 2937–2940.
19 J. Wülfken, PhD Thesis, Hamburg, 2001.
20 H. M. Möller, PhD Thesis, Hamburg, 2003.
21 W. Rasshofer, W. M. Müller and F. Vögtle, *Chem. Ber.*, 1979, **112**, 2095–2119.
22 M. E. Duggan and J. S. Imagire, *Synthesis*, 1989, 131–132.
23 (*a*) M. Mayer and B. Meyer, *Angew. Chem., Int. Ed.*, 1999, **38**, 1784–1788; (*b*) M. Mayer and B. Meyer, *J. Am. Chem. Soc.*, 2001, **123**, 6108–6117; (*c*) R. Meinecke and B. Meyer, *J. Med. Chem.*, 2001, **44**, 3059–3065; (*d*) B. Meyer and T. Peters, *Angew. Chem., Int. Ed.*, 2003, **42**, 864–890.
24 H. Wu, D. G. Myszka, S. W. Tendian, C. G. Brouilette, R. W. Sweet, I. M. Chaiken and W. A. Hendrickson, *Proc. Natl. Acad. Sci. USA*, 1996, **93**, 15030–15035.
25 S. M. Schnittman, H. C. Lane, J. Roth, A. Burrows, T. M. Folks, J. H. Kehrl, S. Koenig, P. Berman and A. S. Fauci, *J. Immunol.*, 1988, **141**, 4181–4186.